Supplemental Information

Fig S1. Schematics of infectivity assays used in this study. CD4 and CCR5 expression levels were determined by flow cytometry using Quantibrite beads. Briefly, 1 x 10^6 cells were stained with anti-CD4 (RPA-T4-phycoerythrin) or anti-CCR5 (2D7-phycoerythrin) (BD Biosciences) at 4°C for 30 min and then fixed with 1.5% formaldehyde. Cell surface staining was analyzed using a FACS CantoII flow cytometer running FACS DiVA software (BD Biosciences). Receptor expression levels were quantified using the QuantiBRITE fluorescence quantitation system (BD Biosciences). Four populations of precalibrated phycoerythrin-conjugated QuantiBRITE beads were processed identically as test samples. Regression analysis was performed on the geometric mean fluorescence intensity of each bead population to estimate antibody molecules bound per cell (ABC) after subtraction of the mean fluorescence intensity of the isotype control.

Fig S2. Clustal Ω alignment of SC45 and PRB958 Env amino acid sequences.

Fig S3. MPEx analysis of MPER mutants. A, NMR structure of MPER peptide (amino acids 662-683; PDB ID 2PV6) in dodecylphosphocholine micelle. The MPER peptide forms a kinked helix in the interfacial region; aromatic and hydrophobic side chains that penetrate into the hydrophobic phase are colored in teal. **B,** WT and Ala-mutated MPER sequences were analysed using the Totalizer function of MPEx (2) to determine the binding free energies (ΔG) of peptides to a phosphatidylcholine interface as well as hydrophobic moment μ_H.

Fig S4. Comparison of V1, V2 and V4 amino acid sequences. X1193.c1 and BG505 HIV-1 share close to 92% sequence homology with SC45 and PRB958 Env sequences, respectively. The V1, V2 and V4 variable domains are aligned and the position of PNGS are numbered and highlighted in green. The glycans in X1193 and BG505 that are in contact between the V1 and V4 loops are indicated above the residues (1). The cysteine residues involved in disulfide bonding are shown in yellow. The SC45-PRB958 P183Q change in V2 is highlighted in pink, while the $D^{186}N^{187}$ deletion in PRB958 is highlighted in grey. The β-sandwich and hairpin loop that is apparently stabilized by the P^{183}-Y^{191} interaction is shown in orange. *nd*: electron density not observed for glycan chain; ***NENQGNRSNNS***, ***TSVQGSNSTGS***: electron density was not observed for these protein segments in BG505. Subtle differences between the V1 loops of X1193.c1 and SC45 as well as BG505 and PRB958 are evident. X1193.c1 contains PNGSs at positions 133, 137 and 142 and an insertion introduces a PNGS after position 138. The V1 loop of SC45 is 5 residues longer, lacks the 133 PNGS but PNGSs at 137 and 142 are conserved; 2 insertions introduce PNGSs after positions 138 and 147. In the cases of BG505 and PRB958, both isolates contain a PNGS at 137, while BG505 contains the 133 glycan and PRB958 has a PNGS-containing insertion after 138. Overall, X1193.c1 and SC45 share 75.2% amino acid identity and 91.6% amino acid homology in the Env ectodomain, while BG505 and PRB958 share 78.9% amino acid identity and 91.1% amino acid homology in the Env ectodomain.

Fig S5. The structures of X1193.c1 (PDB ID 5FYJ) and BG505 (PDB ID 5FYL) SOSIPs (1) were used as models of the V1, V2 and V4 loops of SC45 and PRB958, respectively. The structures of X1193.c1 and BG505 gp120-gp41 heterodimers have been superimposed to highlight their conservation (bottom right). The variable loops (color coded as indicated to left of the structure), are at the apex of the gp120-gp41 spike. The MPER would be located at the base of the spike. The CD4 binding site (CD4bs) is shown in light blue. Asparagine residues forming

part of PNGSs within V1, V2 and V4 are shown as spheres (CPK), while glycan side chains are shown as sticks. The V2-N^{160} glycans forming part of the PG9 epitope are shown. Close-ups of the V1, V2, and V4 loops are shown above the superimposed gp120-gp41 structure. The glycan groups mediating interactions between V1 and V4 are highlighted in dot representation. The structural models were drawn with PyMOL.

Fig S6. Validation of recombinant bNAbs.

A) SDS-PAGE of recombinant bNAbs. Recombinant bNAbs were produced by cotransfection of 293F cells with pCDNA3-based IgG1 heavy and light chains encoding the variable regions of bNAbs 10E8, VRC01 and PGT151. The IgG present in transfection supernatants was adsorbed onto protein G agarose prior to SDS-PAGE in 12% polyacrylamide gels under reducing conditions and Coomassie blue staining. M, molecular weight markers.

B) Specificity of 10E8. 293T cells transfected with WT or F673A-mutated pCDNA3.1-AD8*env* expression vectors or pCDNA3.1 control vector were lysed in PBS containing 1% Triton X100 and 1 mM EDTA. The Env proteins present in cell lysates were captured onto D7324 antibody-coated ELISA plates (AALTO Bio Reagents; directed to A^{497}PTKAKRRVVQREKR at the C-terminus of gp120). The plates were washed, blocked with 10 mg/ml BSA in PBS, and serially diluted bNAbs were then incubated with captured Env proteins. The assays were developed with peroxidase-conjugated rabbit immunoglobulins to human immunoglobulins (DAKO) and 3,3',5,5'-tetramethylbenzidine substrate. F673 is a key component of the 10E8 epitope (3) and substitution of this residue with Ala (F673A) blocks 10E8 binding. VRC01, which is directed to the CD4 binding site, was used to confirm similar coating levels of WT and F673A Envs.

C) Specificity of VRC01. ELISA plates were coated with resurfaced stabilized gp120 core (RSC3) protein or the RCS3 Δ371I mutant. The resurfaced proteins were obtained from Z.-Y. Yang, P. Kwong, G. Nabel and J. Mascola (4) from the NIH AIDS Reagent Program. The ELISA was conducted as above. The Δ371I mutation in the VRC01 epitope ablates VRC01 binding.

D) Specificity of PGT151. HIV-like particles were produced by cotransfecting 293T cells with a pCDNA3-based GagPolVpu expression vector and wild type or N637K-mutated pCDNA3.1-AD8*env* expression vector. HIVLPs were pelleted from culture supernatants through a sucrose/PBS cushion (25% w/v, SW41 rotor, 25,000 rpm, 2.5 h, 4°C). The HIVLPs were resuspended in PBS and then coated onto ELISA plates. The plates were blocked in 5% w/v skim milk powder/PBS and antibody dilutions applied in the presence of 2.5% w/v skim milk powder/PBS. Washing steps were conducted with KPL wash solution lacking detergent. The plates were developed with peroxidase-conjugated rabbit immunoglobulins to human immunoglobulins and 3,3',5,5'-tetramethylbenzidine substrate. To monitor HIVLP coating levels, the HIVLP coated plates were treated with 0.1% Triton X100 at 4°C for 1 h to permeabilize the viral envelope, which is rich in cholesterol and sphingolipids. The anti-capsid monoclonal antibody 183-H12-5C (183) was then used to detect Gag proteins. The ELISA was conducted in the absence of detergents to maintain HIVLP integrity. The N637K mutation has been shown to diminish the neutralization potency of PGT151 (5) and accordingly blocks PGT151 binding to HIVLPs.

References

1. Stewart-Jones, G. B., Soto, C., Lemmin, T., Chuang, G. Y., Druz, A., Kong, R., Thomas, P. V., Wagh, K., Zhou, T., Behrens, A. J., Bylund, T., Choi, C. W., Davison, J. R., Georgiev, I. S., Joyce, M. G., Kwon, Y. D., Pancera, M., Taft, J., Yang, Y., Zhang, B., Shivatare, S. S., Shivatare, V. S., Lee, C. C., Wu, C. Y., Bewley, C. A., Burton, D. R., Koff, W. C., Connors, M., Crispin, M., Baxa, U., Korber, B. T., Wong, C. H., Mascola, J. R., and Kwong, P. D. (2016) Trimeric HIV-1-Env Structures Define Glycan Shields from Clades A, B, and G. *Cell* **165**, 813-826
2. Snider, C., Jayasinghe, S., Hristova, K., and White, S. H. (2009) MPEx: a tool for exploring membrane proteins. *Protein science : a publication of the Protein Society* **18**, 2624-2628
3. Huang, J., Ofek, G., Laub, L., Louder, M. K., Doria-Rose, N. A., Longo, N. S., Imamichi, H., Bailer, R. T., Chakrabarti, B., Sharma, S. K., Alam, S. M., Wang, T., Yang, Y., Zhang, B., Migueles, S. A., Wyatt, R., Haynes, B. F., Kwong, P. D., Mascola, J. R., and Connors, M. (2012) Broad and potent neutralization of HIV-1 by a gp41-specific human antibody. *Nature* **491**, 406-412
4. Wu, X., Yang, Z. Y., Li, Y., Hogerkorp, C. M., Schief, W. R., Seaman, M. S., Zhou, T., Schmidt, S. D., Wu, L., Xu, L., Longo, N. S., McKee, K., O'Dell, S., Louder, M. K., Wycuff, D. L., Feng, Y., Nason, M., Doria-Rose, N., Connors, M., Kwong, P. D., Roederer, M., Wyatt, R. T., Nabel, G. J., and Mascola, J. R. (2010) Rational design of envelope identifies broadly neutralizing human monoclonal antibodies to HIV-1. *Science* **329**, 856-861
5. Falkowska, E., Le, K. M., Ramos, A., Doores, K. J., Lee, J. H., Blattner, C., Ramirez, A., Derking, R., van Gils, M. J., Liang, C. H., McBride, R., von Bredow, B., Shivatare, S. S., Wu, C. Y., Chan-Hui, P. Y., Liu, Y., Feizi, T., Zwick, M. B., Koff, W. C., Seaman, M. S., Swiderek, K., Moore, J. P., Evans, D., Paulson, J. C., Wong, C. H., Ward, A. B., Wilson, I. A., Sanders, R. W., Poignard, P., and Burton, D. R. (2014) Broadly neutralizing HIV antibodies define a glycan-dependent epitope on the prefusion conformation of gp41 on cleaved envelope trimers. *Immunity* **40**, 657-668

FIGURE S1. Schematics of infectivity assays used in this study

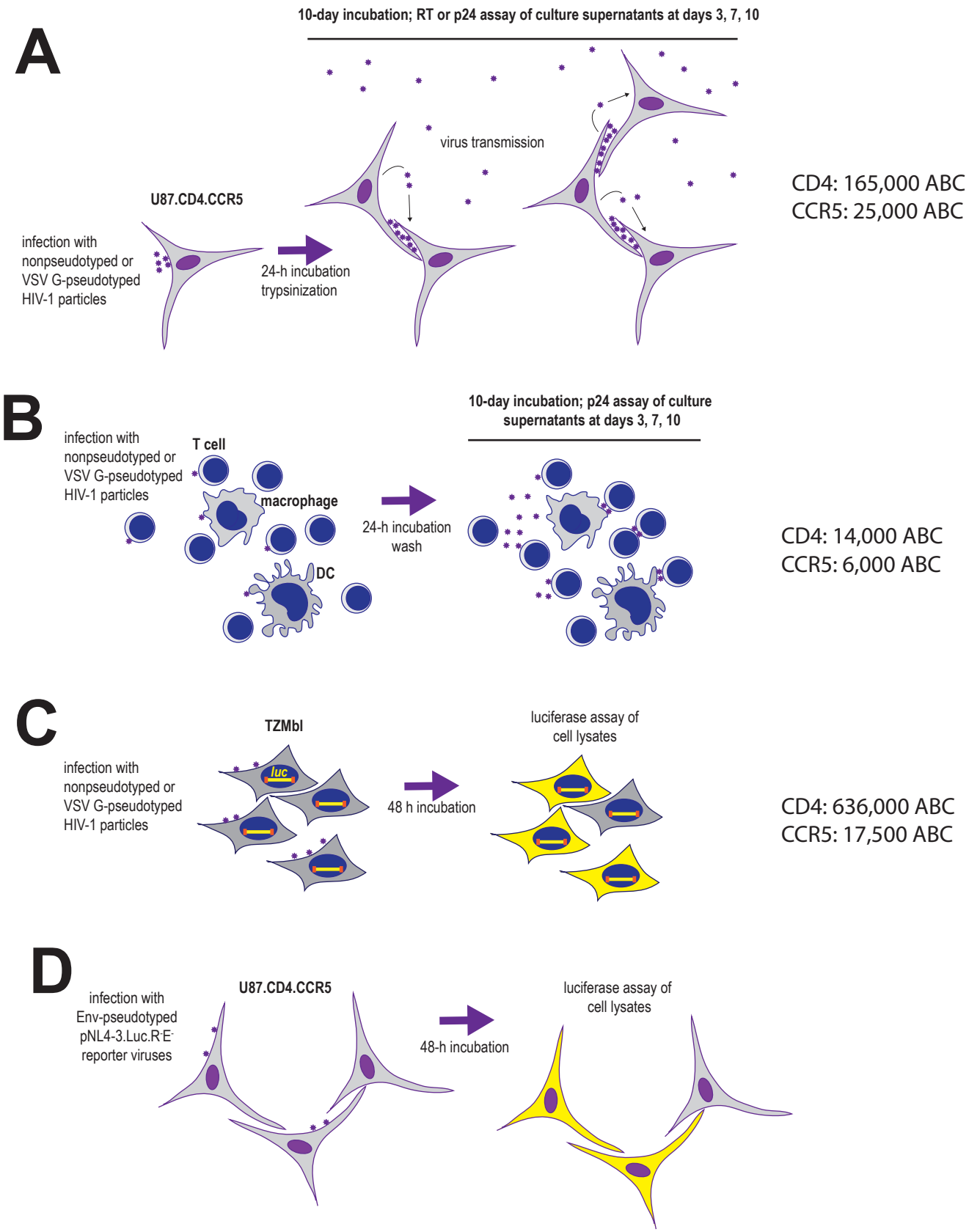

FIGURE S2. Alignment of SC45 and PRB958 Env ectodomain sequences

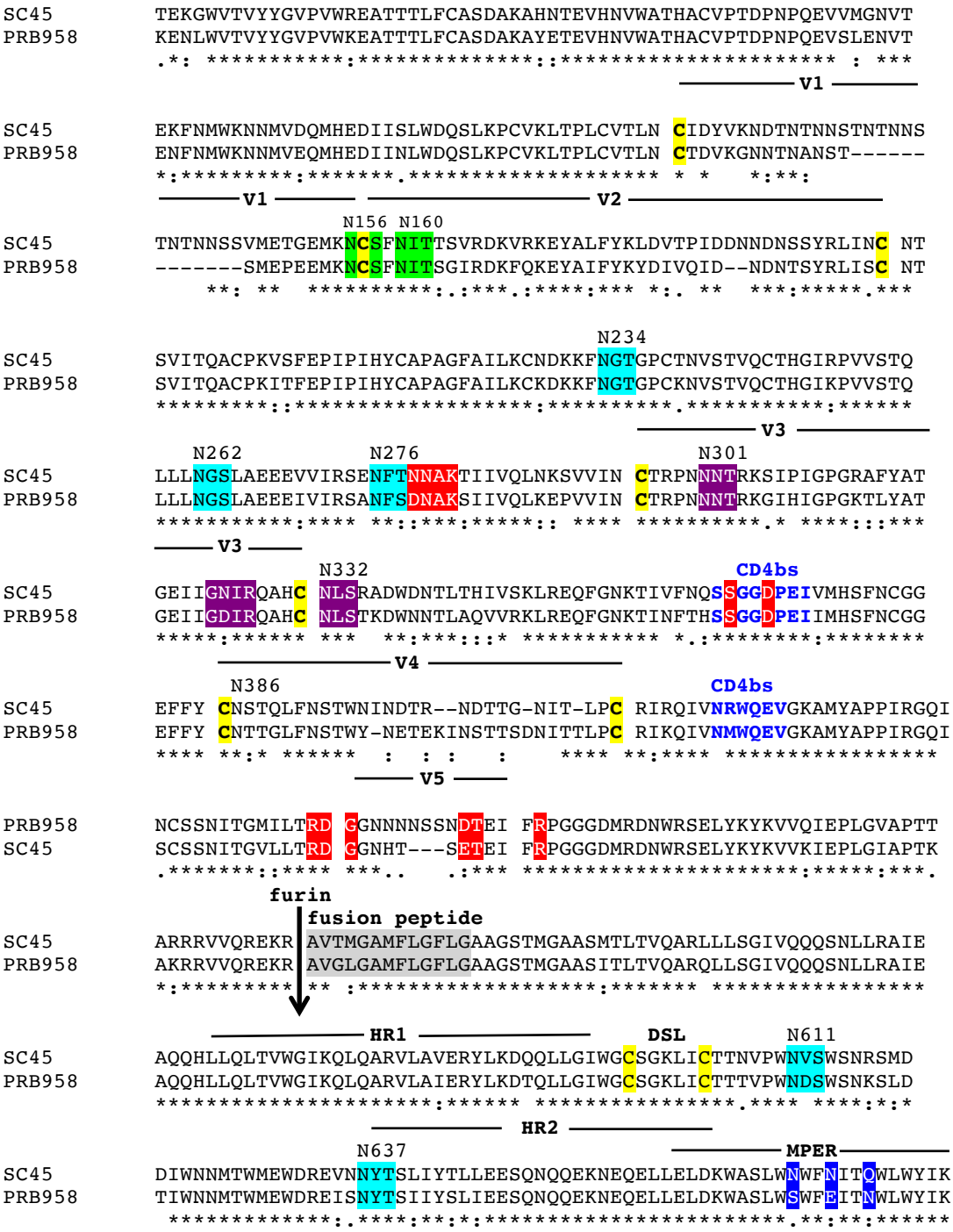

NCS: N-linked glycosylation sites important for PG9 binding
NNT: N-linked glycosylation sites and V3 amino acids important for PGT121 binding
RDG: Amino acids important for VRC01 binding
NYT: N-linked glycosylation sites important for PGT151 binding
C: Cysteines involved in disulfide formation
CD4bs: CD4 binding site
DSL: Disulfide-bonded loop region of gp41
HR1, HR2: Helical regions 1 and 2 of gp41, as defined in the X1193.c1 SOSIP.664 crystal structure (PDB ID 5FYJ)
*, identical amino acids; : ., homologous amino acids; -, deletion

FIGURE S3. Binding free energies of MPER peptides to phosphatidylcholine interfaces.

A

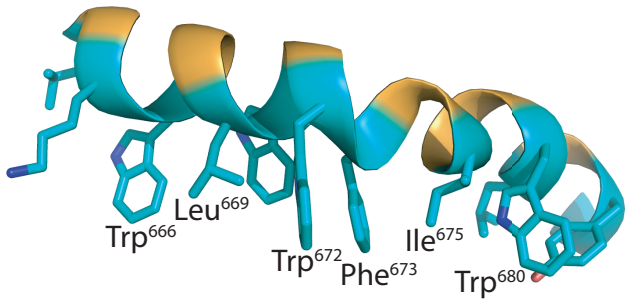

B

E^{662}LDK**W**^{666}ASLWN**W**^{672} FD **I**^{675}TNWLWYIK^{683}

	WT	W666A	W672A	I675A
ΔG	-13.89	-11.87	-11.87	-13.41
μ_H	3.94	2.17	5.65	4.4

FIGURE S4. Comparison of V1V2 and V4 amino acid sequences.

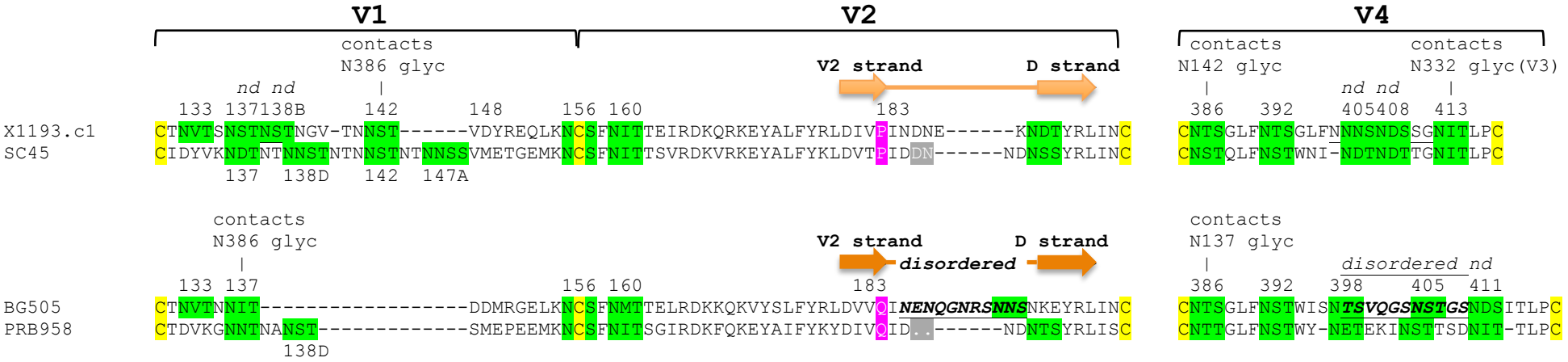

NVT - PNGS
nd - electron density not observed for glycan chain
NENQGNRSNNS*, *TSVQGSNSTGS - electron density not observed for these protein segments in BG505
.. - deleted residues from V2 of PRB958 when compared to SC45

FIGURE S5. X1193.c1 and BG505 SOSIP.664 crystal structures.

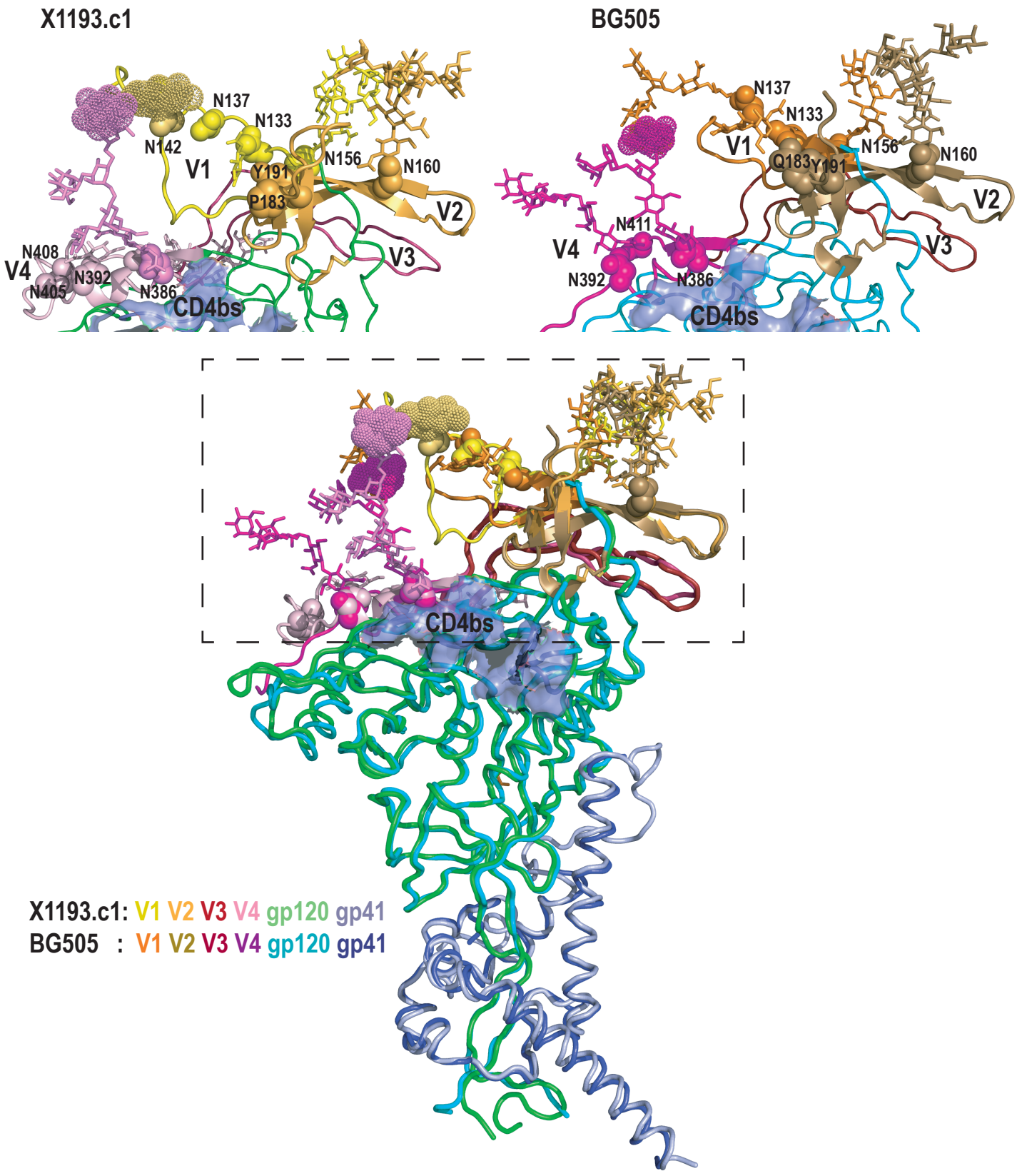

FIGURE S6. Validation of recombinant bNAbs.